

See discussions, stats, and author profiles for this publication at: <https://www.researchgate.net/publication/370314138>

Radiolabeling fingolimod with technetium-99 m and evaluating its biological affinity by in vitro method

Article in Journal of Radioanalytical and Nuclear Chemistry · April 2023

DOI: 10.1007/s10967-023-08907-3

CITATIONS

0

6 authors, including:



Emre Uygur
Ege University

8 PUBLICATIONS 50 CITATIONS

SEE PROFILE



Kadriye Busra Karatay

21 PUBLICATIONS 35 CITATIONS

SEE PROFILE

READS

41



Yasemin Parlak
Manisa Celal Bayar University

45 PUBLICATIONS 267 CITATIONS

SEE PROFILE



Ceren Sezgin
Manisa State Hospital

12 PUBLICATIONS 6 CITATIONS

SEE PROFILE



Radiolabeling fingolimod with technetium-99 m and evaluating its biological affinity by in vitro method

E. Uygun¹ · Y. Parlak² · K. B. Karatay³ · C. Sezgin² · F. G. Gümüşer² · F. Z. Biber Müftüler³

Received: 30 January 2023 / Accepted: 12 April 2023
© Akadémiai Kiadó, Budapest, Hungary 2023

Abstract

Fingolimod (FTY-720) is the first oral medication approved by the food and drug administration (FDA) for the treatment of multiple sclerosis. It acts on the central nervous system by crossing the blood–brain barrier and binding to sphingosine-1-phosphate receptors (S1PRs). FTY-720 protects against neural damage caused by mitochondrial dysfunction and cytotoxicity by modulating S1PR1. In this study, FTY-720 was radiolabeled with technetium-99 m [^{99m}Tc]Tc and the biological affinity of [^{99m}Tc]Tc-FTY-720 was assessed using in vitro methods. The radiochemical yield and stability of [^{99m}Tc]Tc-FTY-720 was over 95% during 4 h. [^{99m}Tc]Tc-FTY-720 showed uptake on the SH-SY5Y cell line.

Keywords Fingolimod · Parkinson's disease · Multiple sclerosis · Technetium-99 m [^{99m}Tc]Tc

Introduction

Parkinson's disease (PD) is the second most common neurodegenerative disease after Alzheimer's disease, affecting approximately six million people worldwide [1]. PD has a positive correlation with age and is more common in male patients [2–4] and its incidence is high (1–3% of the total population) between 65 and 90 years of age. The total number of patients is predicted to increase from 8.7 to 9.3 million by 2030 [5]. PD is currently not a fully curable disease and there is currently no scientifically proven treatment to slow its progression [4, 6]. The symptoms of PD are manifested by dysfunctions of the somatomotor system such as tremors, bradykinesia, and postural instability [1, 2]. On the other hand, the pathological finding in PD is the loss of dopaminergic neurons in the Substantia Nigra pars compacta (SNc) and striatum regions of the brain and the presence of Lewy body bodies containing protein aggregates deposited

in the cytoplasm of the cells [7]. Considering that the loss of dopaminergic neurons continues, early diagnosis of the disease is of great importance. In recent years, there has been an increase in research on the potential for the use of neuroprotective compounds in diagnosing and treating PD [8–15]. Considering the reduction of dopaminergic neurons as the cause of PD, compounds that exhibit neuroprotective effects on these neurons become more important [13, 16].

One of the compounds showing the neuroprotective effect is fingolimod (FTY-720), an analogue of Sphingosine 1-phosphate (S1P) [10–12, 17]. It is a member of the lipid membrane family, which consists of various polar-headed groups such as S1P is expressed by a variety of cells that regulate cell proliferation, differentiation, and survival [3, 18]. FTY-720 is the first oral medication approved by the US Food and Drug Administration (FDA) for the treatment of the relapsing and relapsing form of multiple sclerosis (MS). FTY-720 acts on central nervous system (CNS) cells that cross the blood–brain barrier and express S1P receptors (S1PRs), including neurons [17]. FTY-720 protects against neural damage caused by mitochondrial dysfunction, cytotoxicity, and ischemia–reperfusion injury through modulation of S1PR1 [3, 18, 19]. It has also been reported to be effective against neurodegeneration in PD [3, 11, 12, 18].

A few studies of S1P receptors are radiolabeled with different radionuclides [20–22]. For instance, S1P receptors were radiolabeled with Fluor-18 [¹⁸F] and their usability in positron emission tomography (PET) studies was

✉ E. Uygun
emreuygun2012@gmail.com

¹ Biomedical Device Technologies, Manisa Celal Bayar University, 45140 Yunusemre/Manisa, Turkey

² Department of Nuclear Medicine, Faculty of Medicine, Manisa Celal Bayar University, 45140 Yunusemre/Manisa, Turkey

³ Institute of Nuclear Sciences, Ege University, 35040 Bornova/Izmir, Turkey

investigated [20]. There are also radiolabeling studies with iodine-123 [^{123}I], carbon-11 [^{11}C], and technetium-99 m [$^{99\text{m}}\text{Tc}$] [21–23].

In one of these studies, a new monoclonal antibody imaging probe [$^{99\text{m}}\text{Tc}$]Tc-HYNIC-S1PR1mAb was developed and assessed, to explore the feasibility of targeting the S1PR1 in vitro and in vivo. In this study, S1PR1mAb was equipped and succinimidyl 6-hydraziniumnicotinate hydrochloride was radiolabelled with [$^{99\text{m}}\text{Tc}$]. In vitro studies were carried out to evaluate the binding specificity of [$^{99\text{m}}\text{Tc}$]Tc-HYNIC-S1PR1mAb. The study also performed scintigraphic imaging in mice xenografted with high and low S1PR1 expression. According to the biodistribution study results, there was a significantly higher uptake in SK-HEP-1 tumours than in MCF-7 tumours. On the other hand, reduced uptake of the radiolabeled compound in SK-HEP-1 was observed in tumour-bearing nude mice pre-treated with fingolimod, which binds competitively to the receptors, especially S1PR1. They concluded that [$^{99\text{m}}\text{Tc}$]Tc-HYNIC-S1PR1mAb can be synthesized and specifically targeted to S1PR1 and it has the potential to allow S1PR1 expression assessment with SPECT imaging [23].

[$^{99\text{m}}\text{Tc}$]Tc is an easy, convenient, economical radionuclide used in the development of diagnostic kits in nuclear medicine due to its ideal gamma energy (140 keV) and physical half-life ($t_{1/2} = 6\text{ h}$) [23, 24]. Therefore, approximately 85% of all imaging procedures in nuclear medicine are performed following the administration of radiolabeled compounds with [$^{99\text{m}}\text{Tc}$]Tc [25].

In the current study, fingolimod (FTY-720) was radiolabeled with [$^{99\text{m}}\text{Tc}$]Tc and the biological affinity of the radiolabeled compound ([$^{99\text{m}}\text{Tc}$]Tc-FTY-720) was assessed with in vitro methods.

Experimental

Chemicals and materials

Fingolimod (FTY-720) was purchased from Novartis co. Thin-layer chromatography paper (ITLC-silica), methanol, *N*-octanol, and acetonitrile were purchased from Merck Chemical Co., min. the essential amino acid, Dulbecco's MEM, Min. Essential medium (Mem Eagle), RPMI 1640 Medium, L-glutamine, sodium bicarbonate, sodium pyruvate, fetal bovine serum, penicillin/streptomycin, trypan blue, phosphate buffer solution, trypsin ethylenediamine-tetraacetic acid (EDTA) were purchased from Biological Industries. Technetium-99 m Na) was supplied from Monrol (Eczacibasi, Monrol, Istanbul, Turkey). A low-pressure gradient HPLC system [quaternary pump (LC-10ATvp), diode array detector (DAD; SPD-M20A), NaI(Tl) radioactivity detector (Gabi Star, Raytest), an autosampler (SIL-20A

HT), fraction collector (FRC-10A) and column (RP-C18; 5 μm , 250 \times 4.6 mm I.D., ODS Gl Sciences Inc.)] was used. TLRC measurements were accomplished using a TLC scanner (Bioscan AR-2000 Scanner) and perkin elmer cyclone storage system. Statistical significance was assessed with a one-way analysis of variance and nonlinear regression by the GraphPad program for cell culture studies. The human neuroblastoma cell line (SH-SY5Y) was obtained from the American type culture collection. Cd (Te) detector (Ege University, Institute of Nuclear Science) was used to measure the radioactivity of cells after incorporation studies.

Radiolabeling studies

Radiolabeling conditions with [$^{99\text{m}}\text{Tc}$]Tc radioisotope have been optimized by researchers. Different pH values (3, 5, 7, 9, and 12) have been tested within the scope of optimization studies. In addition, different solvent systems (saline solution, acetonitrile, 9:1 (v/v) methanol–water, 2:8 (v/v) methanol–water) were used. The best result of the pH value is 12 and the solvent system was 9:1 (v/v) acetonitrile–water. Accordingly, 1 mg FTY-720 and $\text{SnCl}_2 \cdot 2\text{H}_2\text{O}$ were dissolved in 1 mL of distilled water, respectively. Then, 25 μg of fingolimod and 25 μg $\text{SnCl}_2 \cdot 2\text{H}_2\text{O}$ were added to a tube and the pH value was brought to 12 with 0.1 M NaOH. [$^{99\text{m}}\text{Tc}$] Na_2TCO_4 (37 MBq) was added to the tube. After, 30 min of incubation was performed at room temperature. Quality control studies of the radiolabeled compound ([$^{99\text{m}}\text{Tc}$] Tc-FTY-720) were carried out by Thin Layer Radio Chromatography (TLRC) and High-Performance Liquid Radio Chromatography (HPLRC) methods.

Quality control studies

Thin layer radio chromatography (TLRC) procedure

The aluminium (ITLC-SG) sheets covered with silica gel (size, 1.50 \times 10 cm- thick, 0.1 mm) and acetonitrile–water (9:1, v/v) solvent system was used. The radiolabeled compound ([$^{99\text{m}}\text{Tc}$]Tc-FTY-720) was dropped on the prepared strips 0.50 cm above the base and counted on the TLRC Scanner (Bioscan AR2000).

High-performance liquid radio chromatography (HPLRC) procedure

HPLRC system with the C18 column was utilized. Researchers optimized HPLC conditions as the mobile phase system Acetonitrile/ dH_2O (v/v, 60:40), the flow rate 1 mL/min. The radioactivity of the radiolabeled compound ([$^{99\text{m}}\text{Tc}$] Tc-FTY-720) was detected using the NaI (Tl) detector (Gabi Star, Raytest) under 254 nm wavelength in the HPLC system.

Stability studies

To determine the stability, the radiolabeled compound was applied to silica strips as in the TLRC procedure at different times (0., 30., 60., 90., 120. and 240. min). Radiochemical yields (%) were examined by the TLRC and the change over time was examined.

Lipophilicity studies

0.3 mL of *n*-octanol and 0.3 mL of pH = 7 buffer were placed in a centrifuge tube, then 0.1 mL of [^{99m}Tc]Tc-FTY-720 was added and the whole mixture was vortexed for 1 min. It was centrifuged at 2500 rpm for 30 min to separate the upper and lower phases. 100 μL samples were taken from each of these phases and counts were taken in the Cd (Te) detector. At the same time, the experimental lipophilicity values obtained were compared with the theoretical lipophilicity values obtained from the ACD/Labs logP Algorithm program (Version 6.0).

Structural analysis

FTY-720 was labelled with inactive Rhenium [^{185}Re] (Re-FTY-720) to determine the possible position of the [^{99m}Tc] Tc in FTY-720. Following this purpose, Rhenium(V)Chloride (Re(V)Cl_3) was dissolved in 1 mL of distilled water. 25 μg of fingolimod and 25 μg $\text{SnCl}_2 \cdot 2\text{H}_2\text{O}$ were added to a tube and the pH value was brought to 12 with 0.1 M NaOH and added 25 μg Re(V)Cl_3 to the tube. 30 min of incubation was performed at room temperature. Then HPLC and $^1\text{H-NMR}$ analyses were performed for Re-FTY-720. HPLC analysis was carried out with the C18 column, Acetonitrile/ dH_2O (v/v, 60:40) mobile phase system. The flow rate was 1 mL/min and UV detections were achieved at 254 nm. The structural analysis of Re-FTY-720 was accomplished by using liquid chromatography- mass spectrometry (LC-MS/MS) method at Manisa Celal Bayar University- applied science research center (ASRC) and nuclear magnetic resonance ($^1\text{H-NMR}$) at Ege University Science and Technology Center (E-BİLTEM).

In Vitro cell culture studies

Human neuroblastoma (SY-SH5Y) cell lines were used in in vitro cell culture studies. SH-SY5Y cells in a medium consisting of minimum Essential Medium (Eagle) and 10% fetal bovine serum (FBS). The cells were incubated in 5% CO_2 and 37 $^\circ\text{C}$. Fresh medium was added by changing the medium every 2 days. After the cells were produced enough to cover 80% of the flasks, they were separated from the flask utilizing a 0.25% (W/V) trypsin-EDTA solution and plated in 24-well plates for incorporation studies and study

groups were formed. The incorporation studies of [^{99m}Tc] Tc-FTY-720 were carried out.

Incorporation studies

SH-SY5Y cells were taken into 24 plates. The time parameters were determined as 30., 60., 120., and 240. min. For SY-SH5Y cells, the existing medium was removed, and a [^{99m}Tc] free medium was placed on the cells in the 24-plate as the control group. Each well on the plates was washed with saline (SF). Medium containing 0.5 mL of radiolabeled (37 MBq) [^{99m}Tc]Tc-FTY-720 was added to each well on the plates. Initial radioactivity (A_0) was determined by counting the radiolabeled medium on the cells in each well at the Cd(Te) detector at 30., 60., 120. and 240 min. To examine the effect of the ligands, the same procedure was applied for free [^{99m}Tc]Tc. The medium was removed from the cells and the wells were washed with 0.5 mL of SF. The radioactivity counts of all radiolabeled samples remaining bound to the cells in the wells were repeated three times. The % binding values were determined by proportioning the detected A_1 and A_0 values and taking the control group counts into consideration. All-time parameters were studied in three repeats ($n = 3$).

Statistical analysis

In the analyses, the average binding values and standard deviations were calculated (3 replicates for each parameter). While evaluating the statistical analysis results of in vitro studies, it was tested whether there was a significant difference at the 95% ($p < 0.05$) confidence level between the intake and uptake values. The P values of the statistical results less than 0.05 were accepted as a significant difference. One-way analysis of variance (ANOVA) was performed with the Graph Pad program for statistical analysis of the data obtained from in vitro cell culture studies. Variance analysis and pearson correlation statistics were performed for these results.

Results and discussion

Radiolabeling

The radiochemical yield of [^{99m}Tc]Tc-FTY-720 was determined by TLRC and HPLRC methods. According to the TLRC chromatograms (Fig. 1), the R_f values of [^{99m}Tc] Tc, Reduced [^{99m}Tc]Tc, and [^{99m}Tc]Tc-FTY-720 were 0.97, 0.26, and 0.84, respectively. On the other hand, the HPLRC chromatograms (Fig. 2), and the retention times of FTY-720, [^{99m}Tc]Tc and [^{99m}Tc]Tc-FTY-720 were 2.11, 6.12 and 2.31 min, respectively (Figure 8). The radiochemical yield

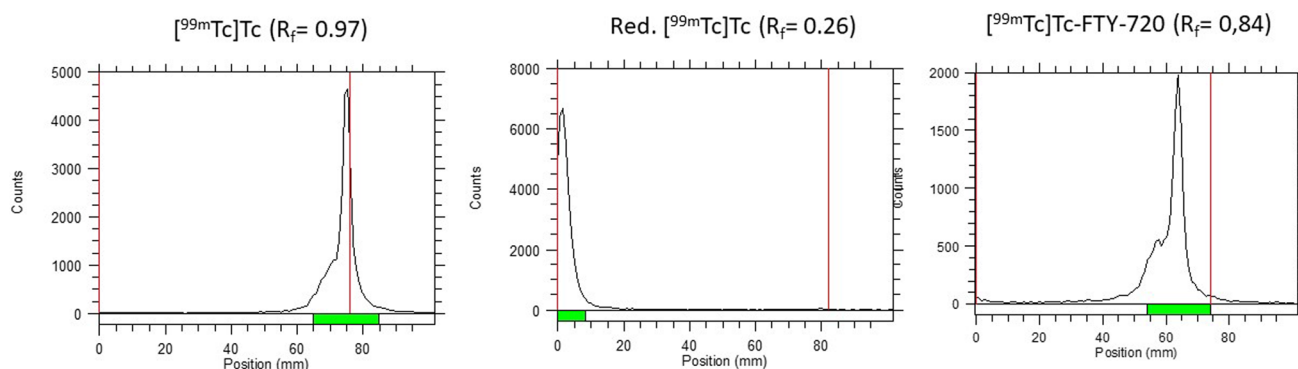


Fig. 1 TLRC Chromatograms of $[^{99m}\text{Tc}]\text{Tc}$, Reduced $[^{99m}\text{Tc}]\text{Tc}$, $[^{99m}\text{Tc}]\text{Tc-FTY-720}$ in the media solution of acetonitrile–water (9:1, v/v)

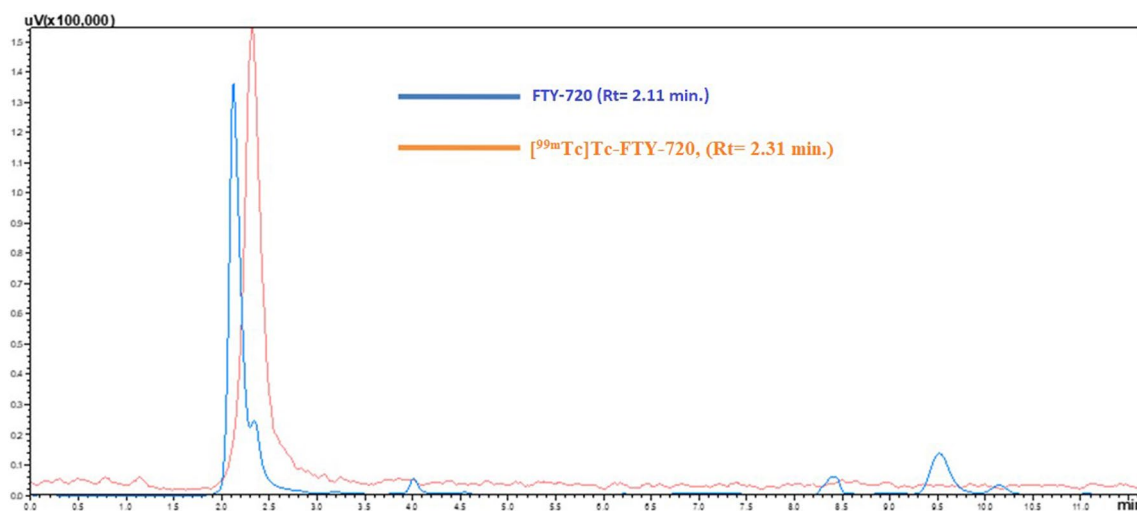


Fig. 2 HPLC Chromatograms of $[^{99m}\text{Tc}]\text{Tc-FTY-720}$

of $[^{99m}\text{Tc}]\text{Tc-FTY-720}$ was over 95% ($\% 98.04 \pm 1.60$, $n=3$). In the literature review, it was found one study about S1P analogues radiolabeling with $[^{99m}\text{Tc}]$ ($[^{99m}\text{Tc}]\text{Tc-HYNIC-S1PR1mAb}$). According to this study, it is seen that the initial radiochemical yield of $[^{99m}\text{Tc}]\text{Tc-HYNIC-S1PR1mAb}$ was $61.45 \pm 9.16\%$, $n=4$. Therefore, purification was done in the PD-10 column, and the radiochemical yield increased by 96.70 ± 0.04 , $n=4$ after the process [23]. Within the scope of the study, FTY-720 was directly radiolabeled with $[^{99m}\text{Tc}]$ and it was determined that the radiochemical efficiency was over 95% ($\% 98.04 \pm 1.60$, $n=3$). This case shows that FTY-720 can be radiolabeled with $[^{99m}\text{Tc}]\text{Tc}$ by a simple system.

Stability

Graph 1 (Fig. 3) is shown the radiochemical yield of the radiolabeled compound versus time. The stability of $[^{99m}\text{Tc}]\text{Tc-FTY-720}$ was over %98 during the 240 min (Graph 1). The results of the serum stability studies demonstrated that

approximately 98% of $[^{99m}\text{Tc}]\text{Tc-FTY-720}$ could exist as an intact complex within 240 min. According to Ye et al., the in vitro stability of $[^{99m}\text{Tc}]\text{Tc-HYNIC-S1PR1mAb}$ reduced from 95 to %85 at the end of 12 h [23]. But the serum stability of $[^{99m}\text{Tc}]\text{Tc-FTY-720}$ was over %98 during the 4 h.

Lipophilicity

Experimental lipophilicity of $[^{99m}\text{Tc}]\text{Tc-FTY-720}$ ($\log P$) was found as 0.48 ± 0.02 , ($n=3$). Also, the theoretical $\log P$ of FTY-720 was calculated as 4.01 ± 0.47 by using the ACD algorithm program (Advanced Chemistry Development, ACD). According to the theoretical $\log P$ value, FTY-720 is lipophilic. Indeed, FTY-720 itself is lipophilic for this it can overcome the blood–brain barrier (BBB). But, activated fingolimod phosphate (FTY-720-P) is a charged ester and is not lipophilic [26]. On the other hand, the lipophilicity of radiolabeled FTY-720 ($[^{99m}\text{Tc}]\text{Tc-FTY-720}$) was decreased in comparison with FTY-720. It is shown that $[^{99m}\text{Tc}]\text{Tc}$

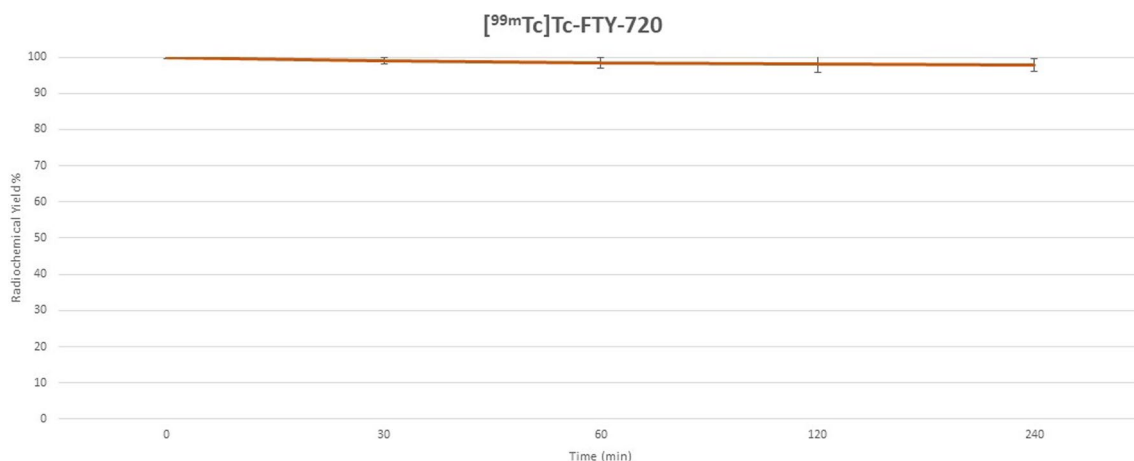


Fig. 3 Stability studies of $[^{99m}\text{Tc}]\text{Tc-FTY-720}$ were assayed by measuring the radiochemical purity at different time

decreased the lipophilicity of the FTY-720. The log P scale of lipophilicity alone for a radiopharmaceutical is not effective in modelling the crossing of any kind of cell membrane like BBB due to large differences in their biophysical properties [27]. For this, further investigation must be carried out.

Characterization

FTY-720 was labelled with inactive Rhenium [^{185}Re] Re (Re-FTY-720) to determine the possible position of the $[^{99m}\text{Tc}]\text{Tc}$ in $[^{99m}\text{Tc}]\text{Tc-FTY-720}$. The inactive form of $[^{185}\text{Re}]\text{Re}$ labelled FTY-720 (Re-FTY-720) was carried out and analyzed to identify the structure of the $[^{99m}\text{Tc}]\text{Tc-FTY-720}$. Figure 4 shows the HPLC chromatogram of Re-FTY-720. The retention times of Re(V) Cl_3 , Re-FTY-720, and FTY-720 were 3.85, 3.89, and

2.43 min, respectively. The molecular formula of the FTY-720 (IUPAC name: 2-amino-2-[2-(4-octyl phenyl) ethyl]propane-1,3-diol) delineated with the ACD/LogP Algorithm software (Version 12.01). The experimental (A) and the two proposed theoretical (B, C) $^1\text{H-NMR}$ spectra of the Re-FTY-720 are seen in Figs. 5 and 6. Table 1 represents the theoretical (according to Fig. 6) and experimental δ (ppm) values of $^1\text{H-NMR}$ (D_2O) for the inactive Re-FTY-720. When the σ (ppm) values are compared between experimental and theoretical $^1\text{H-NMR}$, the first theoretical (C) $^1\text{H-NMR}$ spectra has more possibility because, during radiolabeling studies, the $[^{99m}\text{Tc}]\text{NaTcO}_4$ is reduced to +4 oxidation states with Tin (II) Chloride [28, 29]. LC-MS/MS spectra of the Re-FTY-720 molecule are given in Fig. 7. According to LC-MS/MS results, Re-FTY-720 with 493.67 g/mol molecular weight

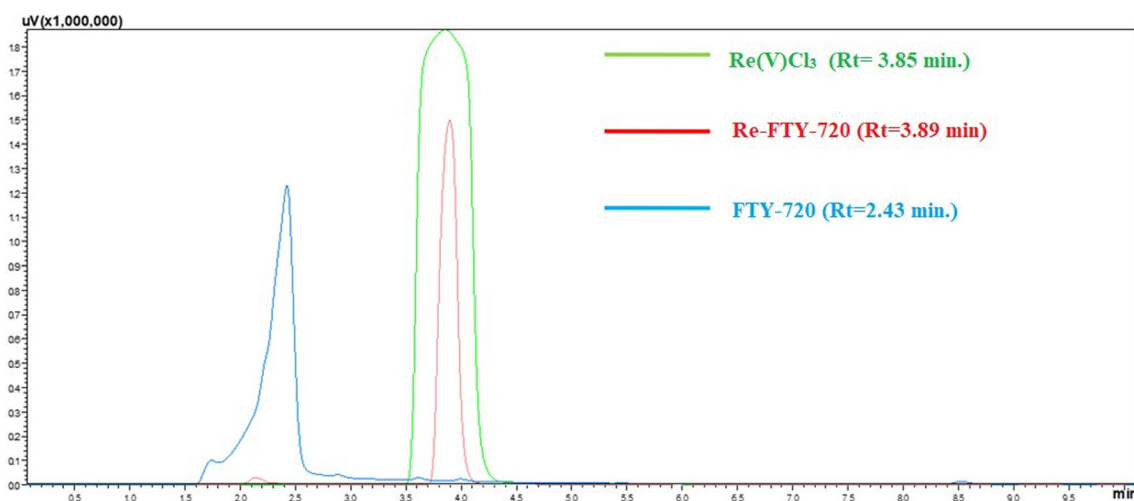


Fig. 4 HPLC Chromatograms of Re(V)Cl_3 , Re-FTY-720 and FTY-720



Incorporation

FTY-720 is an agonist of several S1P receptor subtypes that bind to (S1P) receptors in its phosphorylated state except for S1P2 receptors. The S1P receptor is the regulator of immune cell trafficking, and it is mainly expressed by immune, neural, and endothelial cells, therefore it plays a

Table 1 Theoretical and experimental values of $^1\text{H-NMR}$ for Re-FTY-720

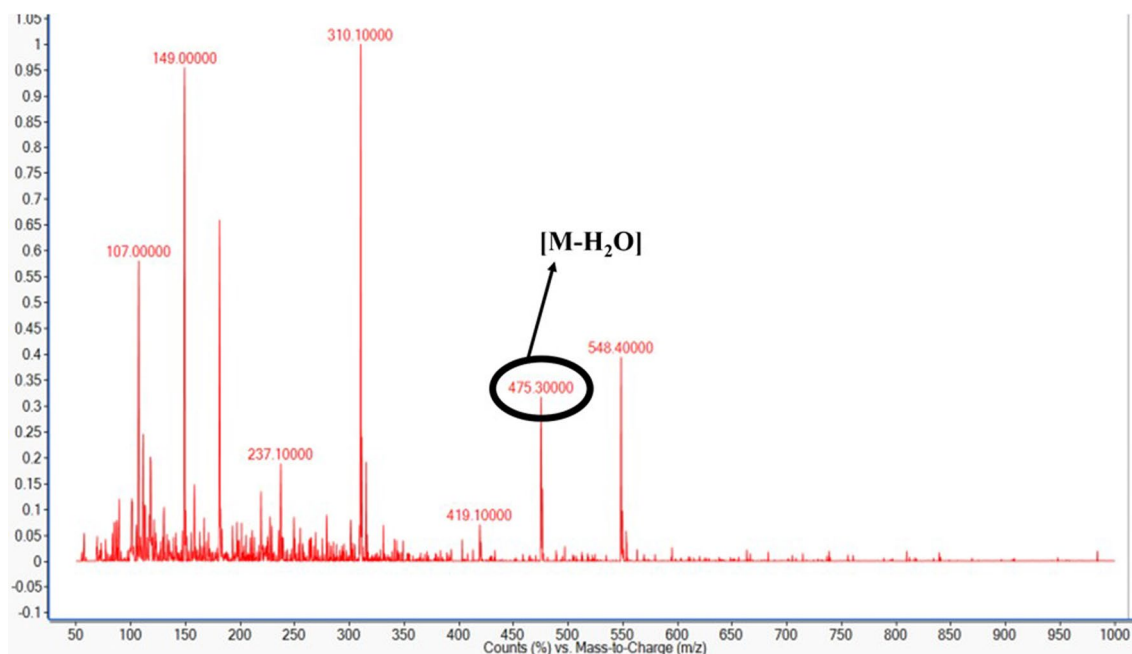
Experimental (A)	Theoretical (B)	Theoretical (C)
σ values (ppm)		
7.88	—	—
7.03–7.13	7.05	7.05–7.26
5.36–5.58	—	—
3.32–3.64	3.59–3.84	3.71–3.84
2.48–2.51	2.55–2.62	2.62–1.80
1.74–1.78	0.88–1.59	1.29–1.31

role in angiogenesis and neurogenesis. The S1P1 receptor is involved in various functions in the CNS, such as neurogenesis, astrocytic activation and proliferation, and communication between astrocytes and neurons and the BBB [30]. FTY-720 treatment regulates the biosynthesis of sphingolipids. So, it plays important role in neurodegenerative diseases such as PD [31]. FTY-720 acts directly on S1PR1-expressed dopaminergic neurons [17]. Within the scope of the study, SH-SY5Y cell lines were used as an in vitro PD model. SH-SY5Y cell lines are often preferred for in vitro PD models. Although some studies have models created using 6-OHDA and rotenone compound using for neurodegenerative effect, most studies consider the SH-SY5Y cell line as a direct PD model [32]. There are several studies on the SH-SY5Y cell line related to FTY-720 [12, 17, 26]. In these studies, it is reported that the FTY-720 compound has neuroprotective and anti-inflammatory effects on the SH-SY5Y cell line. It

is emphasized that FTY-720 has a low cytotoxic effect on the SH-SY5Y cell line, and it has a neuroprotective effect, especially in PD models created using 6-OHDA and rotenone [10, 12]. Within the scope of the study, incorporation studies of the radiolabeled ($^{99\text{m}}\text{Tc}$)Tc-FTY-720) compound on the SH-SY5Y cell line was carried out. Figure 8 shows the incorporation graph of [$^{99\text{m}}\text{Tc}$]Tc-FTY-720 on the SH-SY5Y cell line. The graph shows the binding values of [$^{99\text{m}}\text{Tc}$]Tc and [$^{99\text{m}}\text{Tc}$]Tc-FTY-720 over time in the SH-SY5Y cell line. The binding value of the radiolabelled compound in the SH-SY5Y cell line appears to increase with time from 30. min (18.45 ± 0.92) to 240. min (37.67 ± 1.18). Compared with [$^{99\text{m}}\text{Tc}$]Tc, it was observed that the [$^{99\text{m}}\text{Tc}$]Tc-FTY-720 showed more binding in all time parameters, and the highest binding was at 240 min (37.67 ± 1.18). To sum up, we determined that FTY-720 radiolabeled with [$^{99\text{m}}\text{Tc}$]Tc over 95% radiochemical yields. It has radiochemical stability in serum medium. The radiolabeled compound showed high incorporation values on the SH-SY5Y cell line. Further investigation should be pursued on in vivo PD animal models for a better understanding of the [$^{99\text{m}}\text{Tc}$]Tc-FTY-720 mechanism.

Conclusions

In the current study, Fingolimod was radiolabeled with [$^{99\text{m}}\text{Tc}$] via the direct radiolabeling procedure with higher radiochemical yields. The radiolabeled compound ([$^{99\text{m}}\text{Tc}$]Tc-FTY-720) had stability during the 4 h. The lipophilicity of [$^{99\text{m}}\text{Tc}$]Tc-FTY-720 was decreased in comparison with

**Fig. 7** LC–MS/MS Spectrum of the Re-FTY-720

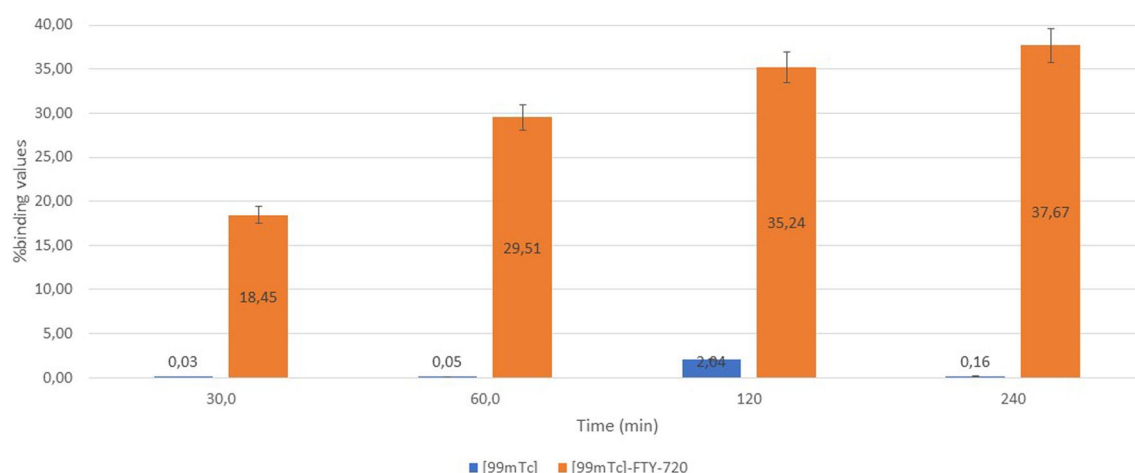


Fig. 8 Time-dependent incorporation graph of [^{99m}Tc]Tc (as control), [^{99m}Tc]Tc-FTY-720 on SH-SY5Y cells

FTY-720. It is shown that [^{99m}Tc]Tc decreased the lipophilicity of the FTY-720. The radiolabelled compound could be encapsulated with poly(lactic-co-glycolic acid) (PLGA) to increase lipophilicity. Furthermore, [^{99m}Tc]Tc-FTY-720 has a considerably high compared to [^{99m}Tc]Tc incorporation efficiency. In conclusion, [^{99m}Tc]Tc-FTY-720 could be a radiolabelled compound that is recommended to be deeply investigated for PD diagnosis, considering its high radiochemical yield, stability and uptake values on SH-SY5Y cells.

Acknowledgements This study is supported by Novartis AG as project number PLSMTA21FEB37 within the scope of For Independent Material Request/Non-Clinical Investigator-Initiated Research program. We also thank Assoc. Prof. Dr Ayfer YURT KILÇAR for her contribution to checking the project proposal.

Declarations

Conflict of interest None of the authors has interest conflict.

References

- Balestrino R, Schapira AH (2020) Parkinson disease. *Eur J Neurol* 27(1):27–42
- Scott LJ (2021) Opicapone: a review in Parkinson's disease. *CNS Drugs* 35(1):121–131
- Vidal-Martinez G, Chin B, Camarillo C, Herrera GV, Yang B, Sarosiek I, Perez RG (2020) A pilot microbiota study in Parkinson's Disease patients versus control subjects, and effects of FTY720 and FTY720-mitox therapy in parkinsonian and multiple system atrophy mouse models. *J Parkinsons Dis* 10(1):185–192
- Peterson DS, Barajas JS, Denney L, Mehta SH (2020) Backward protective stepping during dual-task scenarios in people with Parkinson's disease: a pilot study. *Neurorehabil Neural Repair* 34(8):702–710
- Raza C, Anjum R, Shakeel NA (2019) Parkinson's disease: mechanisms, translational models and management strategies. *Life Sci* 226:77–90
- Delenclos M, Jones DR, McLean PJ, Uitti RJ (2015) Biomarkers in Parkinson's disease: advances and strategies. *Parkinsonism Relat Disord* 22:106–110
- Hernandez LF, Obeso I, Costa RM, Redgrave P, Obeso JA (2019) Dopaminergic vulnerability in Parkinson's disease: the cost of humans' habitual performance. *Trends Neurosci* 42(6):375–383
- Jia D, Deng Y, Gao J, Liu X, Chu J, Shu Y (2014) Neuroprotective effect of Panax notoginseng polysaccharides against focal cerebral ischemia-reperfusion injury in rats. *Int J Biol Macromol* 63:177–180
- Sun A, Xu X, Lin J, Cui X, Xu R (2015) Neuroprotection by saponins. *Phytother Res* 29(2):187–200
- Hoffmann F, Hofreiter J, Rübsamen H, Melms J, Schwarz S, Faber H, Weber P, Pütz B, Loleit V, Weber F, Hohlfeld R, Meinel E, Krumbholz M (2015) Fingolimod induces neuroprotective factors in human astrocytes. *J Neuroinflammation* 12(1):1–13
- Motyl J, Przykaza Ł, Boguszewski PM, Kosson P, Strosznajder JB (2018) Pramipexole and fingolimod exert neuroprotection in a mouse model of Parkinson's disease by activation of sphingosine kinase 1 and Akt kinase. *Neuropharmacology* 125:139–150
- Zhao P, Yang X, Yang L, Li M, Wood K, Liu Q, Zhu X (2017) Neuroprotective effects of fingolimod in mouse models of Parkinson's disease. *FASEB* 31(1):172–179
- Panahi Y, Rajaei SM, Johnston TP, Sahebkar A (2019) Neuroprotective effects of antioxidants in the management of neurodegenerative disorders: a literature review. *J Cell Biochem* 120(3):2742–2748
- Mamun AA, Hashimoto M, Hossain S, Katakura M, Arai H (2014) Neuroprotective effect of madecassoside evaluated using amyloid B 1–42-mediated in vitro and in vivo Alzheimer's disease models neuroprotective effect of madecassoside evaluated using amyloid β 1–42 -mediated in vitro and in vivo Alzheimer's disease. *Int J Indig Med Plants* 47:1669–1682
- Kandil EA, Sayed RH, Ahmed LA, Abd El Fattah MA, El-Sayeh BM (2018) Modulatory role of Nurr1 activation and thrombin inhibition in the neuroprotective effects of dabigatran etexilate in rotenone-induced Parkinson's disease in rats. *Mol Neurobiol* 55(5):4078–4089

16. Garlapati PK, Raghavan AK, Shivanna N (2014) Phytochemicals having neuroprotective properties from dietary sources and medicinal herbs. *Pharmacognosy J* 7(1):1–17
17. Bascuñana P, Möhle L, Brackhan M, Pahnke J (2020) Fingolimod as a treatment in neurologic disorders beyond multiple sclerosis. *Drugs R and D* 20(3):197–207
18. Sardoiwala MN, Karmakar S, Choudhury SR (2020) Chitosan nanocarrier for FTY720 enhanced delivery retards Parkinson's disease via PP2A-EzH2 signalling in vitro and ex vivo. *Carbohydr Polym* 254:117435
19. Sivasubramanian M, Kanagaraj N, Dheen ST, Tay SSW (2015) Sphingosine kinase 2 and sphingosine-1-phosphate promote mitochondrial function in dopaminergic neurons of a mouse model of Parkinson's disease and in MPP+-treated MN9D cells in vitro. *Neuroscience* 290:636–648
20. Prasad VP, Wagner S, Keul P, Hermann S, Levkau B, Schäfers M, Haufe G (2014) Synthesis of fluorinated analogues of sphingosine-1-phosphate antagonists as potential radiotracers for molecular imaging using positron emission tomography. *Bioorg Med Chem* 22(19):5168–5181
21. Liu H, Jin H, Yue X, Han J, Baum P, Abendschein DR, Tu Z (2017) PET study of sphingosine-1-phosphate receptor 1 expression in response to vascular inflammation in a rat model of carotid injury. *Mol Imag* 16:1–7
22. Rosenberg AJ, Liu H, Jin H, Yue X, Riley S, Brown SJ, Tu Z (2016) Design, synthesis, and in vitro and in vivo evaluation of an ^{18}F -labeled sphingosine 1-phosphate receptor 1 (S1P1) PET tracer. *J Med Chem* 59(13):6201–6220
23. Ye M, Gai Y, Ji H, Jiang Y, Qiao P, Wang W, Zhang Y, Xia X, Lan X (2021) A novel radioimmune $^{99\text{m}}\text{Tc}$ -labeled tracer for imaging sphingosine 1-phosphate receptor 1 in tumor xenografts: an in vitro and in vivo study. *Front Immunol* 12:1–9
24. Vermeulen K, Vandamme M, Bormans G, Cleeren F (2019) Design and challenges of radiopharmaceuticals. *Semin Nucl Med* 49(5):339–356
25. Kar NR (2019) Production and applications of radiopharmaceuticals: a review. *Int J Pharm Investig* 9(2):36–42
26. Hunter SF, Bowen JD, Reder AT (2016) The direct effects of fingolimod in the central nervous system: implications for relapsing multiple sclerosis. *CNS Drugs* 30(2):135–147
27. Liu X, Testa B, Fahr A (2011) Lipophilicity and its relationship with passive drug permeation. *Pharm Res* 28(5):962–977
28. Biber Muftuler FZ, Unak P (2017) A perspective on $^{99\text{m}}\text{Tc}$ and $^{125}/^{131}\text{I}$ labelled receptor targeted compounds and their in vitro/ in vivo affinities. *J Radioanal Nucl Chem* 314(19):1–6
29. Volkov MA, Novikov AP, Grigoriev MS, Fedoseev AM, German KE (2022) Novel synthesis methods of new imidazole-containing coordination compounds Tc(IV, V, VII) —reaction mechanism, Xrd and hirshfeld surface analysis. *Int J Mol Sci* 23(16):452
30. Brinkmann V (2007) Sphingosine 1-phosphate receptors in health and disease: mechanistic insights from gene deletion studies and reverse pharmacology. *Pharmacol Ther* 115(1):84–105
31. Czubowicz K, Jęsko H, Wencel P, Lukiw WJ, Strosznajder RP (2019) The role of ceramide and sphingosine-1-phosphate in Alzheimer's disease and other neurodegenerative disorders. *Mol Neurobiol* 56(8):5436–5455
32. Falkenburger BH, Schulz JB (2006) Limitations of cellular models in Parkinson's disease research. *J Neural Transm Suppl* 70:261–268

Publisher's Note Springer Nature remains neutral with regard to jurisdictional claims in published maps and institutional affiliations.

Springer Nature or its licensor (e.g. a society or other partner) holds exclusive rights to this article under a publishing agreement with the author(s) or other rightsholder(s); author self-archiving of the accepted manuscript version of this article is solely governed by the terms of such publishing agreement and applicable law.